Behavior of chemically powered Janus colloids in lyotropic chromonic liquid crystal

Devika Gireesan Sudha[1],Hend Baza[2],David P. Rivas[3],Sambeeta Das[3],Oleg D. Lavrentovich[2],Linda S. Hirst[1],
[1]*Department of Physics, University of California Merced, Merced, CA 95343, USA*
[2]*Liquid Crystal Institute and Chemical Physics Interdisciplinary Program, Kent State University, Kent, OH 44242, USA and*
[3]*Department of Mechanical Engineering, University of Delaware, Newark, DE 19716, USA**

(Dated: April 25, 2024)

Platinum-coated Janus colloids exhibit self-propelled motion in aqueous solution via the catalytic decomposition of hydrogen peroxide. Here, we report their motion in a uniformly aligned nematic phase of lyotropic chromonic liquid crystal, disodium cromoglycate (DSCG). When active Janus colloids are placed in DSCG, we find that the anisotropy of the liquid crystal imposes a strong sense of direction to their motion; the Janus colloids tend to move parallel to the nematic director. Motion analysis over a range of timescales reveals a cross-over from ballistic to anomalous diffusive behavior on timescales below the relaxation time for liquid crystal elastic distortions. Surprisingly we observe that smaller particles roll during ballistic motion, whereas larger particles do not. This result highlights the complexity of phoretically-driven particle motion, especially in an anisotropic fluid environment.

I. INTRODUCTION

Active fluids are out-of-equilibrium systems composed of active elements (particles, rods etc.) suspended in a fluid medium. These active elements transduce energy from their environment into autonomous motion, causing the fluid to exhibit rich dynamic behavior. Such behavior can include collective motion [1–3], motility-induced phase separation [4, 5], flow instabilities, and pattern formation [6–8]. Several recent studies have focused on the behavior of active colloids dispersed in isotropic fluids, including self-assembly and their collective dynamics [9–11]. A relatively unexplored direction in this field, concerns the replacement of the suspending fluid by a non-Newtonian anisotropic fluid, a nematic liquid crystal. Liquid crystals (LCs) are elastic fluids with some degree of anisotropy. They have long-range molecular orientational order, and the direction of average molecular ordering is given by a director, $\hat{\mathbf{n}}$. A spherical colloid immersed in a uniformly aligned nematic LC will locally perturb the nematic director field as determined by the particle surface anchoring and Frank elasticity [12–14].

In this paper, we report on the behavior of individual active Janus colloids in a nematic liquid crystal. The anisotropic nematic phase is an interesting environment for studying active colloids, since it exhibits both anisotropic viscosity and Frank elasticity [14–16]. For this work, we selected chemically powered synthetic active colloids driven by a surface chemical reaction. Common propulsion mechanisms for active Janus colloids include self-diffusiophoresis or self-electrophoresis. Such mechanisms result from asymmetric catalytic reactions on their surfaces that generate gradient-driven fluid flows around the colloids, propelling them forward [17, 18]. We used Janus colloids fabricated with platinum (Pt) - capped polystyrene (PS) spheres, that exhibit self-propelled motion in aqueous hydrogen peroxide (H_2O_2) solution via catalytic decomposition into water and oxygen. These Janus colloids typically propel with the PS side leading the way. The Pt-Janus particles were originally thought to propel by means of self-diffusiophoresis [19], whereby a local concentration gradient is established through the catalytic reaction on the Pt surface. The precise mechanism has however been a recent subject of debate. Observations of ionic effects influencing propulsion direction have indicated electrophoretic contributions to the motion [20, 21]. The liquid crystal host in our experiments, was carefully selected as disodium cromoglycate (DSCG), a chromonic lyotropic liquid crystal with a nematic phase at room temperature [22]. This material provides an aqueous environment compatible with the hydrogen peroxide-powered Janus particles. DSCG was recently used to investigate the motion of bacteria in liquid crystal. Remarkably, at very low bacterial concentrations, Zhou et al. [23] introduced a novel class of active matter – the living liquid crystal - induced by the activity of bacteria moving in passive liquid crystal. These living liquid crystals, exhibit chaotic dynamics and motile topological defects, strikingly similar to the dynamic characteristics of microtubule-based active nematics [24]. Inspired by these results, we focused on the dynamics of individual active Janus colloids in nematic liquid crystal, as a synthetic analog to the bacterial system [23]. Elucidating the fundamentals of Janus particle motion in a liquid crystal environment represents the first step towards studying their collective motion.

In our experiments, DSCG was aligned by treating the bounding glass substrates with polyimide SE-7511, to give a planar director orientation [25]. This configuration allowed easy observation of particle position and orientation using fluorescence microscopy. The liquid crystal phase was visualized using crossed polarizers on an optical microscope, revealing liquid crystal distortion profiles around the particles. Tracking the motion of Janus col-

* lhirst@ucmerced.edu

loids revealed that liquid crystal anisotropy significantly influenced their trajectories. Particles tended to move parallel to the direction of average molecular ordering defined by the director. Our analyses reveal that motion profiles are characterized by a combination of anomalous diffusion and ballistic behavior. We also observed the Janus colloids rolling while moving in DSCG, despite no significant change in their direction of motion.

II. EXPERIMENTAL METHODS

A. Janus Colloid Preparation

Janus colloids were prepared by coating polystyrene microspheres with platinum (Pt) using electron beam (e-beam) deposition. Polystyrene paramagnetic microspheres (Cospheric Inc.) were selected as the base particles. Before coating the colloids with a metal layer, they were first diluted in ethanol and then spread evenly on a glass slide. Once dried, the colloids were coated by e-beam deposition with 3 nm of Nickel (Ni) followed by 30 nm of Pt. The Ni layer was added to make the colloids magnetic in order to potentially explore how magnetic torques would affect the colloid's behavior, although such experiments were not part of the current study. The colloids were then removed from the slide using a small piece of wet lens tissue gently dragged over the slide to pick up the colloids. The tissue was then placed in a plastic 1.5 mL tube containing approximately 0.5 mL of de-ionized water and the was tube shaken and vortexed before removing the tissue. The finished particles were characterized using scanning electron microscopy (SEM) with a ZEISS Gemini SEM 500 instrument. Figure 1a shows an SEM image of two particles, the conductive hemisphere (lighter) is clearly visible for each (scale bar = 2 μm).

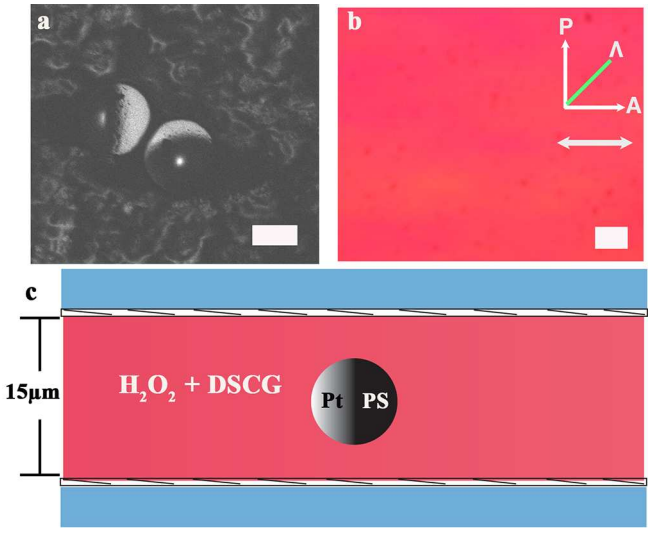

FIG. 1. Materials and methods. a) SEM image, captured with backscattered electron detection mode, of 4 μm sized fluorescent microspheres (excitation 510 nm, emission 550 nm) half coated with Pt. Scale bar = 2 μm. b) Polarized microscopy image of uniformly aligned DSCG inside a pre-assembled cell of thickness 15 μm. Imaged using a full wave (λ) retardation plate, as imdicated by the green line. Polarizer (P) and Analyser (A) directions are also indicated. Scale bar = 2 μm. c) Cross-sectional schematic of the experimental cell containing DSCG, H_2O_2 and a Janus particle.

B. Liquid Crystal Cell Preparation

We worked with two different Janus colloid diameters, 4.0 μm and 11.8 μm. From a stock solution containing colloids of each respective size, 5 μL was pipetted and re-suspended in 30% H_2O_2 aqueous solution, to a final 20% H_2O_2 concentration. This solution was then sonicated before mixing with liquid crystal. Initially the Pt coating on the particle is quite reactive, generating significant O_2 bubbles. This is a greater problem for the larger particles. Bubbles make colloid visualization difficult and form many air-liquid interfaces that influence particle trajectories, so we aimed to minimize their production. To minimize O_2 bubbles for each particle size, we optimized the wait time after the initial addition of H_2O_2 solution to the particle suspension - 1 hr for the 4.0 μm Janus colloids and 3 hrs for the 11.8 μm Janus colloids. After these respective wait times, 1 μL of a control particle solution (polystyrene divinylbenzene, DVB spheres, 6 μm diameter, 0.5 mg/mL) was also added to the Janus/ H_2O_2 solutions. A mixture of DSCG (Sigma Aldrich) at 25 wt% in de-ionized water was prepared, then subsequently diluted to 15.38 wt% (to be in the nematic phase) by adding 5 μL of the prepared Janus/H_2O_2 solution. This method produced a final 7.21% concentration of H_2O_2, enough for activity, while minimizing oxygen bubbles. To further minimize the effect of bubbles causing advective flows, the Janus + DSCG + fuel solution was loaded into the pre-assembled cell after an additional waiting time. One hour for the 4 μm Janus colloids and 6 hrs for the 11.8 μm colloids. The cell was constructed from two parallel glass plates (20 mm x 10 mm) separated by 15 μm spacers. The interior surfaces of the glass plates were pre-treated with polyimide SE-7511 [25] and rubbed with a velvet cloth to produce unidirectional planar anchoring. Figure 1b shows an optical microscope image of an uniformly aligned cell filled with DSCG. After loading, the cell was sealed with epoxy glue and placed flat on the microscope stage to minimize gravitational effects due to tilt. Proper cell sealing and placement on the stage were important to minimize drift during imaging. The absence of drift was verified using DVB spheres. The cells were imaged with polarized optical microscopy (POM) using a Leica DM2500P upright microscope with a HI PLAN 40x/0.65 objective lens. Videos were recorded at 1 frame per second over a period of 8 min using a color camera [Basler Ace 2.3 MP]. Figure 1c shows a diagram of the experimental cell.

C. Particle tracking and Image analysis

Janus colloids were tracked spatially from fluorescence microscopy images using Trackpy – a python package which locates Gaussian blob-like features in video images, follows them through time and records their trajectories [26]. Tracking yields x, y coordinates for each colloid as a function of i, the frame number. The liquid crystal was imaged between crossed polarizers with a full wave retardation plate. Figure 1b, shows an example image of an aligned DSCG nematic phase with the director, polarizer and retardation plate directions indicated.

III. RESULTS AND DISCUSSION

A. Director distortions around Janus colloids

Experiments were performed on 4.0 μm and 11.8 μm diameter Janus colloids, recording the behavior of individual active particles in a uniaxially aligned nematic using optical imaging. When colloidal particles are immersed in liquid crystal, anisotropic molecular interactions with the surface of the colloid cause elastic distortions in the surrounding director field. Depending on the size and shape of the colloid as well as on the strength and type of anchoring at the colloidal surface, these distortions can be of dipolar or quadrupolar symmetry [27]. We first investigated the nature and scale of local nematic distortions around Janus colloids with no activity using POM imaging.

Figure 2 (a-f) & (g-o) respectively show two different Janus particle sizes (4 μm and 11.8 μm) inside an aligned nematic phase of DSCG, imaged under different modes. The different Janus configurations highlighted here are i) full-moon – where the Pt metallic cap on one side is facing down, maximum brightness; ii) half-moon – where both sides of the Janus are showing, half bright, and iii) new-moon – where the metallic cap is facing up, minimum brightness. Figure 2 (a-c) shows a 4 μm diameter Janus colloid in the full moon configuration imaged under three different modes. The POM image (Figure 2b) shows a weakly distorted nematic around the colloid with quadrupolar symmetry. But close observation by inserting a full-wave retardation plate between the crossed polarizers (Figure 2c) reveals slight yellow tinges around the particle, signaling that the nematic distortions on each side of the colloid are locally chiral. This chiral nature becomes a little more obvious in the half-moon configuration (Figure 2 d-f). A larger colloid with similar anchoring causes longer-range distortions in the nematic director, making optical observations easier. Observations of the 11.8 μm diameter Janus colloid (Figure 2, g-o) show the same local chirality. Using passive spherical DVB colloidal particles with tangential surface anchoring in the same liquid crystal, Á. T. Martínez et al [28] observed two energetically distinct helical distortions, class-1 & class-2. These distortions consist of twisted tails that extend away from the particle parallel to the far-field nematic director. This behavior can be understood because DSCG has an unusually small twist elastic modulus making twist distortions energetically cheap [29]. This property allows the director to spiral around the central axis of the colloid leading to twisted tails that extend much farther away from the particle than the splay and bend distortions of pure quadrupoles. Figure 2 shows that we observe the same director configuration with 4 μm and 11.8 μm Janus colloids consistent with a class-1 localized helical distortion [28]. In a class-1 elastic distortion the director spirals around the central axis in the same sense on opposite sides of the colloidal particle. It is a chiral dipole, characterized as an elastic multipole with both quadrupolar and chiral dipolar terms. These results suggest that, despite the Janus particle's inherently different hemispherical sides, anchoring around the colloid is tangential.

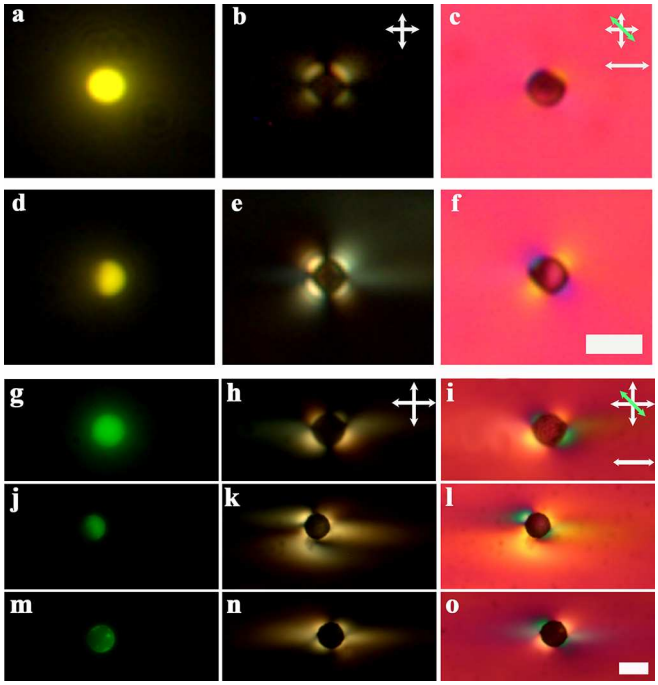

FIG. 2. Distortion around inactive Janus colloid inside an aligned cell at different Janus configurations. Microscope images of 4 μm Janus particle inside 18 μm thick cell in full moon (a,b,c,) and half-moon (d,e,f) configurations under different imaging modes. a,d) Fluorescence microscopy images. b,e) crossed-polarized microscopy images. c,f) crossed-polarized microscopy images with an inserted full wave retardation plate (green arrow). Scale bar = 5 μm. Microscopy images of 11.8 μm Janus particle inside 30 μm thick cell in full moon (g,h,i), half-moon (j,k,l) and new moon (m,n,o) configurations under different imaging modes. g,j,m) Fluorescence microscopy images. h,k,n) crossed-polarized microscopy images. i,l,o) crossed-polarized microscopy images with an inserted full wave retardation plate (green arrow). Scale bar = 10 μm. Magnification 63x water immersion, NA = 0.9

We quantified the twisted tail lengths for the particles in Figure 2 using the method described in [28]. For the 4 μm Janus particle in full-moon, the distortions were too weak to identify the intensity spread along the equatorial plane. Comparatively, for the half-moon, tail lengths are asymmetric on the sides and ~ 5.65 μm. Similarly in the case of the 11.8 μm Janus particle, the tail lengths are asymmetric on the sides and are ~ 30.00 μm, 43.51 μm and 41.84 μm for the full-moon, half-moon and new-moon configurations respectively. Therefore the tail lengths are observed to vary with colloid size (consistent with [28]) and Janus configuration.

B. Effect of liquid crystal on Janus colloid motion

In a simple aqueous H_2O_2 solution, Pt-coated Janus colloids undergo self-propulsion. We performed a series of experiments to quantify their transport. As controls, we also studied their behavior under two different scenarios: in water with no fuel, (Figure 3a), and in water with fuel (7.21% peroxide solution), (Figure 3b). With no fuel, the Janus colloids exhibit characteristic Brownian motion, with an average displacement of 7 μm in 5 min (Figure 3a). In the presence of fuel, the Janus colloids become active and exhibit enhanced Brownian motion with a directional component to their motion, and an average displacement of 35 μm in 10 min (Figure 3b and supplemental video S1). These control results were compared with motion in the nematic phase of DSCG in the presence of fuel (7.21% peroxide concentration), (Figure 3c). Strikingly, when introduced to the uniaxially aligned liquid crystal, in the presence of fuel, the Janus colloids show ballistic behavior. The anisotropy of the liquid crystal phase guides the Janus particles to swim along the nematic director. In Figure 3c and supplemental video S2, the DSCG nematic director is oriented at 45°with respect to the analyzer, and we see the active Janus colloid self-propels in a direction close to that of the nematic director. This Janus colloid has an average displacement of 26 μm after 8min in DSCG. While catalytic decomposition of H_2O_2 on the Pt-side of the Janus colloid powers its motion, the liquid crystal renders directionality. This is the first report of chemically-powered synthetic Janus particles moving in a liquid crystal environment. Motion profiles of the Janus particles were analyzed by plotting the mean square displacement (MSD) of the particles as a function of time (See appendix). Figure 3d shows MSD plots for 10 different 4 μm-diameter active Janus particles (represented by dotted lines) moving in DSCG. The particles were each tracked for 8 min at 1 frame per second (fps) and their motion plotted on a log-log scale. The solid magenta line represents the average of all 10 trajectories. A linear fit to this average produces a slope of 1.98 $\pm$ 0.01 indicating that motion is predominantly ballistic throughout the time of observation. Within a lag time of 480s (period of observation), 4 μm diameter Janus particles were observed to travel distances ranging from 24 μm – 90 μm. These differences are likely due to variation in the amount of fuel around different particles. Once the Pt + H_2O_2 reaction fuel fully depletes, the Janus particles behave like passive colloids.

C. Anisotropic and anomalous motion of active Janus colloids

In prior experiments with active bacteria moving in DSCG [23], the preferred direction of motion was observed to be parallel to the director. To investigate the directional preference of a single active Janus colloid, we calculated MSDs parallel and perpendicular to the director. MSDs, averaged over 10 active Janus colloids, clearly show that motion parallel to the far-field director is substantially longer than motion perpendicular to the director (Figure 3e). We can understand this behavior by considering the anchoring around the colloids which causes asymmetric director field distortions (Figure 2) and an effective anisotropic viscosity. The director field distortion (twisted tails) is elongated along the overall far-field director leading to different effective viscosities for colloidal motion parallel and perpendicular to the director. Such viscoelastic effects have been shown to favor particle displacement along the director [30]. In our case, we did observe some translation perpendicular to the director, but $MSD_{\parallel}$ is significantly larger than $MSD_{\perp}$.
In addition to their anisotropic motion over long timescales, we also observed that the colloids exhibit anomalous diffusion when the time step between particle position measurements was 0.05s. In this experiment, five different active Janus colloids (4 μm in diameter) moving in DSCG inside a cell of thickness 15 μm were recorded for 5 mins at 0.05s time steps. Trajectories for analysis were obtained by splitting the 5 min long video into tracks of duration 1 min. A time averaged MSD calculation was performed on each 1min track. Then an ensemble average was taken by averaging over these 1 min trajectories. As Janus particles are moving in an anisotropic environment, motion parallel and perpendicular to the director were calculated separately (Figure 3f). The MSD curves reveal two regimes of motion – a regime with a smaller slope at short lag times that slowly transitions into a steeper slope at longer lag times. The crossover time for $MSD_{\parallel}$ corresponds to $t_{\parallel} = 0.79$s with a slope of 1.14 ± 0.02 at $t < t_{\parallel}$ and 1.95 ± 0.01 at $t > t_{\parallel}$. The crossover time for $MSD_{\perp}$ is at $t_{\perp} = 1.39$s with a slope of 1.09 ± 0.01 at $t < t_{\perp}$ and 1.85 ± 0.01 at $t > t_{\perp}$. At short lag times, the 4 μm active Janus particle tends to both diffuse, and to move in a straight line. Whereas at longer lag times, they exhibit ballistic behavior. T. Turiv et al [30] reported anomalous sub-diffusive behavior for tangentially anchored passive silica spheres at time scales comparable to the characteristic relaxation time $\tau \sim \frac{\eta l^2}{K}$ of the director perturbations around the sphere. In this formula, l is the characteristic length of the director dis-

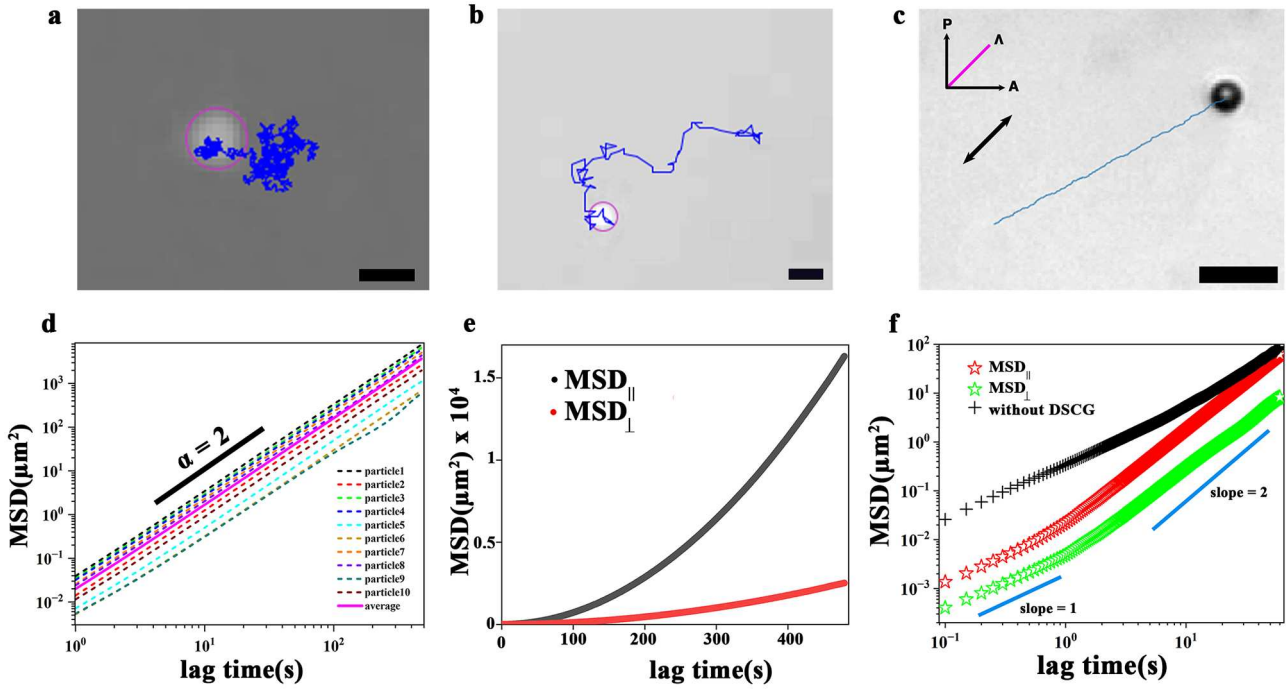

FIG. 3. Motion analysis of 4 μm-diameter individual Janus particles. a) Trajectory of an inactive Janus colloid in water recorded for 5 mins at 50 fps. Scale bar = 5 μm b) Trajectory of an active Janus colloid in 7.21% H_2O_2 solution captured for a duration of 10 min at 0.2 fps. Scale bar = 5 μm. c) Trajectory of an active Janus colloid in DSCG inside an aligned pre-assembled cell recorded for 8 min at 1 fps. Scale bar = 10 μm. d) Mean squared displacement (MSD) plots on a logarithmic scale, of individual active Janus colloids moving in uniformly aligned DSCG inside a cell of thickness 15 μm and captured at 1 fps for 8 min. e) MSD plots calculated parallel and perpendicular to the director, averaged over 10 different active Janus colloids moving in DSCG inside an aligned cell of thickness 15 μm, captured for 8min at 1fps. f) MSD plots of active Janus colloids in the presence and absence of DSCG recorded for 1 min at 20 fps.

tortion relaxing back to equilibrium, η is the rotational viscosity, which we estimated to be ~ 0.2 Pa.s [31] and K is the Frank elastic constant. Assuming $l = 1$ μm for the class 1, active Pt- coated Janus sphere with a configuration specific distortion profile and twist elastic constant of DSCG at 23 °C [29], τ was found to be ~ 0.29s. This τ value is slightly less than the crossover time, below which anomalous diffusive behavior was observed. Besides the propulsive thrust from the catalytic breakdown of H_2O_2, active particles also face a elastic relaxation force from the liquid crystal that slows down propulsion at short time steps. However, the same MSD curve calculated in water (with H_2O_2 but no liquid crystal), showed no crossover between slopes (Figure 3f black crosses). This highlights the role played by liquid crystal in steering the Janus particle and rendering ballistic motion.

D. Rolling

Video analysis reveals the rolling behavior of 4 μm active Janus particles as they move in DSCG (Figure 4). In this figure we contrast the typical behavior of a 4 μm particle with a larger, 11.8 μm diameter particle. The 4 μm Janus particle undergoes rolling, exhibiting different moon phases (Figure 4a), with the intensity graph showing peaks and valleys. A peak corresponds to a full moon configuration and a valley indicate a new moon configuration. The 11.8 μm particle, on the other hand, does not roll, with a constant intensity profile (Figure 4b). Before discussing these results, it is important to consider possible mechanisms for particle rolling.

Active particles move via self-generated phoretic mechanisms in the presence of fuel and the motion occurs in general, due to the interaction of self-generated fields with the interfacial boundary region of the particle. The particle/liquid crystal interfacial boundary layer is a very thin region of the surrounding fluid much less than the size of the particle. A self-generated field around the particle can consist of a solute concentration gradient, set up by the catalytic chemical reaction on the Pt side, or an electric field generated by proton currents at the Pt end that emanate from the vicinity of the equator and end near the pole [20]. These fields create a local pressure imbalance leading to an effective slip velocity along the interfacial boundary layer, driving fluid flows [18, 32–34]. The self-phoretic effective slip velocity, v_s, induced by the solute concentration field, C, along the interface can be written as $v_s = \mu \nabla_{\parallel} C_s$ [32]. Here, μ is the characteristic diffusiophoretic mobility and $\nabla_{\parallel} C_s$ is the tangential

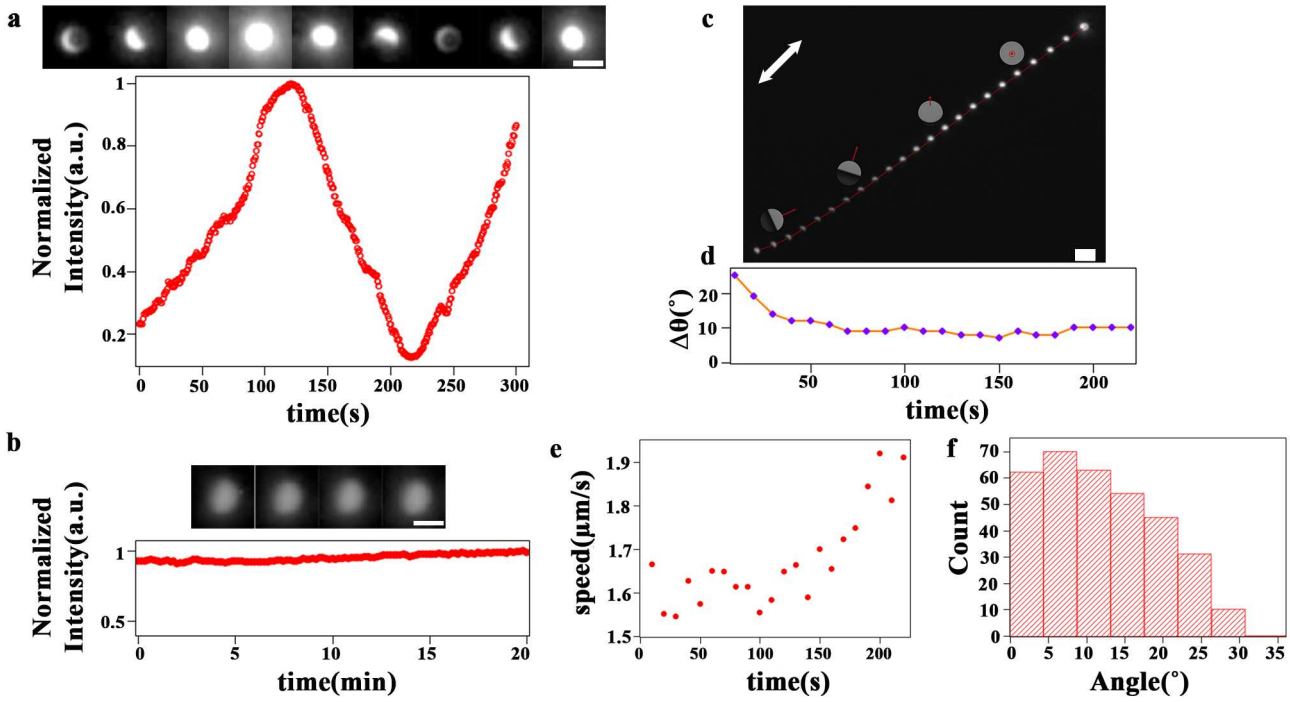

FIG. 4. Rolling of small Janus particles while moving in a uniformly aligned DSCG. a) Fluorescence microscopy images capturing the moon phases of a 4 μm active Janus particle inside a 18 μm cell for a duration of 5 min and corresponding intensity plots of the of the same Janus particle demonstrating rolling. Scale bar = 5 μm. b) Fluorescence microscopy images of 11.8 μm active Janus particle inside a 30 μm cell recorded over a duration of 20 min and corresponding intensity plot demonstrating the absence of rolling over the period of observation. Scale bar = 10 μm. c) Composite image showing the curved trajectory of a rolling 4 μm Janus particle inside a 15 μm DSCG cell, captured every 10s for 220s. Scale bar =10 μm. d) Graph of $\Delta\theta$, the deviation in direction of motion with respect to the nematic director orientation, e) speed, with time for the particle depicted in (c). f) Histogram of $\Delta\theta$ values that active 4 μm Janus particles take while moving in DSCG observed for a duration of 220s at every 10s interval, calculated for seven different particles.

gradient of C at the outer limit of the boundary layer. While considering self-propulsion through electrokinetic effects, μ is replaced with the zeta potential, ζ and C with a self-generated electric field, ψ [34]. Any spatial non-uniformity in the mobility constant caused by fabrication defects, can lead to a rotational component of the effective slip velocity. The particle velocity will be proportional to the sum of the mobilities, and angular velocity is proportional to the difference between the mobilities on the two sides [35]. We expect the particle to turn and align its axis of symmetry along the field gradient. This would mean that after adopting this configuration (for example PS side first), rolling should cease. In our case we observe something different. The particles continue to rotate throughout their tracked trajectories, and do not reach an orientational equilibrium (Figure 4c). To try to explain this phenomenon, we can consider the effects of a spatially varying fuel concentration field. Such a variation would add polar and azimuthal components to the local slip velocities at the particle surface, greatly complicating determination of the particle mobility [34, 35].

In water (Figure 3b), Janus particles can exhibit spiral trajectories, due to their non-uniform surface properties [36, 37]. When such particles are placed in an aligned liquid crystal, the combination of an off-center propulsive force and elastic restoring forces due to the liquid crystal environment can lead to a slightly curved trajectory, or linear propulsion in a direction slightly different to the nematic director. In Figure 4c, we can see a Janus particle moving in aligned DSCG, with the nematic director indicated by a double headed arrow. The particle begins its path in the half-moon configuration, then rolls to adopt a full moon configuration and continues forward. The corresponding deviation in particle trajectory with respect to the nematic director ($\Delta\theta$) is plotted in Figure 4d. While in the half-moon configuration, $\Delta\theta$ is high, then the particle rolls, and $\Delta\theta$ drops to $\sim 10°$. We observe a rise in velocity (Figure 4e) as the Janus particle trajectory comes more in alignment with the nematic director. Figure 4f shows a histogram of $\Delta\theta$s calculated for 7 different active Janus particle trajectories. The most common trajectory direction, $\Delta\theta$ was in the range 4.4°-8.8°. As particles move in DSCG, we typically observe some curvature in their trajectories – they don't always move in a straight line while propelling close to the director orientation.

This behavior is very non-intuitive, based on the simpli-

fied picture of Janus particle propulsion. It should be noted that the behavior of each Janus particle moving in DSCG is, to some extent, unique. Although general behaviors can be obtained, the surface chemical properties of each particle can vary from spot to spot. Adding to this, possible spatial non-uniformity of the fuel environment around the colloid, makes each Janus particle different. In addition to these local effects, global inhomogenities in the fuel concentration field further complicate the behavior. Under these conditions, rolling behavior can be considered stochastic over long timescales.

In Figure 4c and in supplemental video S3, we see a fascinating result - the particle rolls with no change in its direction of motion. Considering that particle propulsion occurs in general due to catalytic breakdown of H_2O_2 on the particle's Pt side [18–21], there are two important things to note. First, surface chemical activity – how quickly a concentration gradient can be set-up by the chemical reaction and second, the surface phoretic mobility – how effectively the surface interacts with this gradient to generate fluid flows [37]. S. Ebbens et al. [20] reported particle motion as a combination of neutral and ionic diffusiophoresis as well as electrophoretic effects whose interplay can be varied through ionic effects such as pH and salt concentration. DSCG is a disodium salt and high salt concentrations are known to reduce the turnover rate of H_2O_2 [20]. Moreover, the characteristic diffusion time of reaction products (O_2, H_3O^+) around the Janus colloid (4 μm) is $\tau_d = \frac{R^2}{D}$, where $D = \frac{k_B T}{6\pi\eta a}$ depends on the rotational viscosity of DSCG and the radius of the product particle, a [38]. τ_d for O_2 and H_3O^+ $\sim$ equals 0.55s and 0.37s respectively. These, and our results suggest that while the rotational configuration of the Janus takes time to react to the fuel and set-up a gradient, the existing gradient may give enough thrust to push the particle forward.

Finally, we observed that the large colloids (11.8μm in diameter) don't roll while moving in DSCG, (Figure 4b) and tend to move much closer to the director. This can be understood as they create a larger elastic distortion in the surrounding liquid crystal (Figure 2), and in general move much more slowly. In addition, because their distortion profiles are sensitive to particle orientation, rolling for larger particles becomes increasingly energetically expensive. This behavior might also be related to elastic levitation as descibed by O. P. Pishnyak *et al* [39] where elastic repulsion from the bounding substrates keeps the colloid in the nematic bulk, mediated by director distortions. A large colloid is repelled more strongly from the substrates than a small colloid, thus a larger colloid is often levitating near the midplane of the cell. This leads to just a small difference in shear stresses above and below the colloid and therefore suppresses rolling.

IV. CONCLUSIONS

In this paper, we report the directed movement of synthetic, chemically powered active Janus particles in a liquid crystal nematic phase. Examination of individual particle trajectories reveals some surprising behaviors. Particle motion is governed by liquid crystal anisotropy, but is also strongly influenced by asymmetries in the individual particles. The particle motion, while close to ballistic over longer timescales, is influenced by the significant, orientation-dependent director distortions around the particle. In addition, non-uniformities in metallic cap coatings and fuel concentration have non-trivial effects on particle propulsion direction and anomalous rolling behaviors. Achieving passive control over simple synthetic active particles is an important goal in the field of active matter, and one that might lead to new ways of achieving collective control. By studying the basic behaviors of anisotropic fluid on single Janus colloids our work helps to lay the foundation for these future directions.

ACKNOWLEDGMENTS

This work was supported by the generous funding from the National Science Foundation (NSF) award DMR-2104574, NSF-CREST: Center for Cellular and Biomolecular Machines at University of California Merced (NSF-HRD-1547848 and NSF-HRD-2112675) and UC Mexus-CONACYT collaborative grant CN-20-142. The authors would also like to acknowledge Jeremias Gonzalez and Patrick Noerr, from University of California Merced, for their inputs and helpful discussions relating to this work.

Appendix A: Twisted tail length

To calculate the tail length, we used crossed-polarized microscopy images of 4 μm & 11.8 μm Janus colloids (Figure 2). Prior to calculation, the images were converted into 8-bit. As demostrated in the supplemental material of [28] intensity profile was plotted for a line along the equatorial plane. The resulting decaying intensity tails were fitted with the Gaussian peak equation,

$$I = I_0 + \frac{A}{w}\sqrt{\frac{2}{\pi}}\exp\left(-2\left(\frac{x - x_c}{w}\right)^2\right)$$

and length was estimated using the Full Width at Half Maximum (FWHM) concept. In the above equation, the width parameter w is related to the standard deviation σ by $\sigma = \frac{w}{2}$. This gives a FWHM = $\sqrt{2\ln 2}w$ representing the length of intensity spread around the object. We take the average of the decaying intensity tails on the two sides to find the tail length.

Appendix B: Mean squared displacement (MSD)

MSD curves for each individual particle track defined by {x(i), y(i)} were calculated using a method described in reference [40]. The MSD, for a given time lag t, is defined as the average over all pairs of points separated by that time lag using,

$$\langle \Delta r^2(t) \rangle = \frac{\sum_{i=1}^{N_i} [(x(t_i + t) - x(t_i))^2 + (y(t_i + t) - y(t_i))^2]}{N_i}$$

In this definition, t_i is the time for the i^{th} image in the track and N_i represents the number of images over which the average is calculated.

Appendix C: Intensity analysis

The fluorescence microscopy videos show a bright feature (the fluorescent side of the Janus colloid) moving in time against a black background. To characterize the orientation of the colloid we took advantage of the fact that only one hemisphere (the non-metallic side) is fluorescent. By observing a single particle, the total integrated intensity in every video frame was obtained using Trackpy [26]. Maximum intensity in this case corresponds to a full moon configuration – when the metallic cap is facing down and the fluorescently labelled polystyrene half is facing up. A minimum intensity corresponds to a new moon configuration – when the metallic cap is facing up and the fluorescently labelled polystyrene half is facing down. To normalize these integrated intensities, the intensity of each frame in a video was divided by (I_{max}), the maximum observed integrated intensity.

Appendix D: $\Delta\theta$ analysis

To measure how much the direction of motion of active colloid deviates from the nematic director orientation, we calculated $\Delta\theta = \Delta\theta_{LC} - tan^{-1}(\frac{dy}{dx})$, where $\Delta\theta_{LC}$ is the nematic director orientation (in our case 45°) and dx, dy are the displacements of active Janus moving in liquid crystal along x, y directions respectively.

[1] J. Toner, Y. Tu, and S. Ramaswamy, Hydrodynamics and phases of flocks, Annals of Physics **318**, 170 (2005), special Issue.

[2] S. Ramaswamy, The mechanics and statistics of active matter, Annual Review of Condensed Matter Physics **1**, 323 (2010).

[3] T. Vicsek and A. Zafeiris, Collective motion, Physics Reports **517**, 71 (2012).

[4] M. E. Cates and J. Tailleur, Motility-induced phase separation, Annu. Rev. Condens. Matter Phys. **6**, 219 (2015).

[5] C. Bechinger, R. Di Leonardo, H. Löwen, C. Reichhardt, G. Volpe, and G. Volpe, Active particles in complex and crowded environments, Reviews of Modern Physics **88**, 045006 (2016).

[6] R. A. Simha and S. Ramaswamy, Hydrodynamic fluctuations and instabilities in ordered suspensions of self-propelled particles, Physical review letters **89**, 058101 (2002).

[7] D. Saintillan and M. J. Shelley, Instabilities, pattern formation, and mixing in active suspensions, Physics of Fluids **20** (2008).

[8] X. Fu, L.-H. Tang, C. Liu, J.-D. Huang, T. Hwa, and P. Lenz, Stripe formation in bacterial systems with density-suppressed motility, Physical review letters **108**, 198102 (2012).

[9] W. Wang, W. Duan, S. Ahmed, A. Sen, and T. E. Mallouk, From one to many: Dynamic assembly and collective behavior of self-propelled colloidal motors, Accounts of chemical research **48**, 1938 (2015).

[10] I. S. Aranson, Active colloids, Physics-Uspekhi **56**, 79 (2013).

[11] S. A. Mallory, C. Valeriani, and A. Cacciuto, An active approach to colloidal self-assembly, Annual review of physical chemistry **69**, 59 (2018).

[12] P.-G. de Gennes and J. Prost, *The physics of liquid crystals* (Oxford university press, 1993).

[13] P. Poulin, H. Stark, T. Lubensky, and D. Weitz, Novel colloidal interactions in anisotropic fluids, Science **275**, 1770 (1997).

[14] I. I. Smalyukh, Liquid crystal colloids, Annual Review of Condensed Matter Physics **9**, 207 (2018).

[15] H. Stark, Physics of colloidal dispersions in nematic liquid crystals, Physics Reports **351**, 387 (2001).

[16] O. D. Lavrentovich, Design of nematic liquid crystals to control microscale dynamics, Liquid crystals reviews **8**, 59 (2020).

[17] K. K. Dey and A. Sen, Chemically propelled molecules and machines, Journal of the American Chemical Society **139**, 7666 (2017).

[18] J. L. Moran and J. D. Posner, Phoretic self-propulsion, Annual Review of Fluid Mechanics **49**, 511 (2017).

[19] J. R. Howse, R. A. Jones, A. J. Ryan, T. Gough, R. Vafabakhsh, and R. Golestanian, Self-motile colloidal particles: from directed propulsion to random walk, Physical review letters **99**, 048102 (2007).

[20] S. Ebbens, D. Gregory, G. Dunderdale, J. Howse, Y. Ibrahim, T. Liverpool, and R. Golestanian, Electrokinetic effects in catalytic platinum-insulator janus swimmers, Europhysics Letters **106**, 58003 (2014).

[21] A. Brown and W. Poon, Ionic effects in self-propelled pt-coated janus swimmers, Soft matter **10**, 4016 (2014).

[22] N. Zimmermann, G. Jünnemann-Held, P. J. Collings, and H.-S. Kitzerow, Self-organized assemblies of colloidal particles obtained from an aligned chromonic liquid crystal dispersion, Soft Matter **11**, 1547 (2015).

[23] S. Zhou, A. Sokolov, O. D. Lavrentovich, and I. S. Aranson, Living liquid crystals, PNAS **111**, 1265 (2014).

[24] A. J. Tan, E. Roberts, S. A. Smith, U. A. Olvera, J. Arteaga, S. Fortini, K. A. Mitchell, and L. S. Hirst,

Topological chaos in active nematics, Nature Physics **15**, 1033 (2019).

[25] Y. A. Nastishin, H. Liu, T. Schneider, V. Nazarenko, R. Vasyuta, S. Shiyanovskii, and O. D. Lavrentovich, Optical characterization of the nematic lyotropic chromonic liquid crystals: Light absorption, birefringence, and scalar order parameter, Physical Review E **72**, 041711 (2005).

[26] D. B. Allan, T. Caswell, N. C. Keim, C. M. van der Wel, and R. W. Verweij, soft-matter/trackpy: v0. 6.1, Zenodo, Feb (2023).

[27] I. Muševič, *Liquid crystal colloids*, Vol. 530 (Springer, 2017).

[28] A. Martinez, P. J. Collings, and A. Yodh, Brownian dynamics of particles "dressed" by chiral director configurations in lyotropic chromonic liquid crystals, Physical review letters **121**, 177801 (2018).

[29] S. Zhou, K. Neupane, Y. A. Nastishin, A. R. Baldwin, S. V. Shiyanovskii, O. D. Lavrentovich, and S. Sprunt, Elasticity, viscosity, and orientational fluctuations of a lyotropic chromonic nematic liquid crystal disodium cromoglycate, Soft Matter **10**, 6571 (2014).

[30] T. Turiv, I. Lazo, A. Brodin, B. I. Lev, V. Reiffenrath, V. G. Nazarenko, and O. D. Lavrentovich, Effect of collective molecular reorientations on brownian motion of colloids in nematic liquid crystal, Science **342**, 1351 (2013).

[31] H. Baza, T. Turiv, B.-X. Li, R. Li, B. M. Yavitt, M. Fukuto, and O. D. Lavrentovich, Shear-induced polydomain structures of nematic lyotropic chromonic liquid crystal disodium cromoglycate, Soft Matter **16**, 8565 (2020).

[32] J. L. Anderson, Colloid transport by interfacial forces, Annual review of fluid mechanics **21**, 61 (1989).

[33] Y. Ibrahim, R. Golestanian, and T. B. Liverpool, Multiple phoretic mechanisms in the self-propulsion of a pt-insulator janus swimmer, Journal of Fluid Mechanics **828**, 318 (2017).

[34] R. Golestanian, T. Liverpool, and A. Ajdari, Designing phoretic micro-and nano-swimmers, New Journal of Physics **9**, 126 (2007).

[35] T. Bickel, G. Zecua, and A. Würger, Polarization of active janus particles, Physical Review E **89**, 050303 (2014).

[36] X. Wang, M. In, C. Blanc, A. Wurger, M. Nobili, and A. Stocco, Janus colloids actively rotating on the surface of water, Langmuir **33**, 13766 (2017).

[37] B. W. Longbottom and S. A. Bon, Improving the engine power of a catalytic janus-sphere micromotor by roughening its surface, Scientific Reports **8**, 4622 (2018).

[38] R. Golestanian, Anomalous diffusion of symmetric and asymmetric active colloids, Physical review letters **102**, 188305 (2009).

[39] O. P. Pishnyak, S. Tang, J. Kelly, S. V. Shiyanovskii, and O. D. Lavrentovich, Levitation, lift, and bidirectional motion of colloidal particles in an electrically driven nematic liquid crystal, Physical review letters **99**, 127802 (2007).

[40] M. A. Catipovic, P. M. Tyler, J. G. Trapani, and A. R. Carter, Improving the quantification of brownian motion, American Journal of Physics **81**, 485 (2013).